

Controlling the complex Lorenz equations by modulation

G. Kociuba* and N. R. Heckenberg

Department of Physics, University of Queensland, St Lucia, Queensland, Australia

(Received 25 March 2002; published 12 August 2002)

We demonstrate that a system obeying the complex Lorenz equations in the deep chaotic regime can be controlled to periodic behavior by applying a modulation to the pump parameter. For arbitrary modulation frequency and amplitude there is no obvious simplification of the dynamics. However, we find that there are numerous windows where the chaotic system has been controlled to different periodic behaviors. The widths of these windows in parameter space are narrow, and the positions are related to the ratio of the modulation frequency of the pump to the average pulsation frequency of the output variable. These results are in good agreement with observations previously made in a far-infrared laser system.

DOI: 10.1103/PhysRevE.66.026205

PACS number(s): 05.45.Ac

I. INTRODUCTION

Chaotic behavior occurs widely in nonlinear systems. Investigation of general properties of such systems have shown that there are features such as unstable periodic orbits and routes to chaos, which are common in all chaotic systems. This has opened up the possibility that there may be generic ways to control such systems to periodic behavior, in spite of their individual differences. Current methods of control of chaos rely on the idea that a chaotic system has an attractor that is wound around an infinite number of unstable periodic orbits [1]. Control is achieved when one of those orbits is stabilized. One method of control is to apply feedback to a chaotic system, e.g., the Ott, Grebogi, and Yorke method [2]. This has the advantage that only a relatively small perturbation, determined by the state of the chaotic system, is required to control a chaotic system. A disadvantage of this method and its variations is the requirement that the computation time for the control algorithm must be faster than the average period of the chaotic system. There also exist non-feedback control methods, where the applied perturbation of an accessible parameter is independent of the state of the system. This perturbation can be noise [3], chaotic [4] or periodic [5]. We have previously shown that our ammonia ring laser operating in the autonomous chaotic regime could be controlled to periodic pulsations by modulation of the pump power [6]. We found control to different periods, and that the locking ratios between the pump modulation frequency and the laser intensity output pulsation frequency was not restricted to one-to-one. Here we investigate the effect of applying a periodic modulation to one of the system parameters of the complex Lorenz equation in the chaotic regime. We choose these equations because it has been shown to be a simplified model of a traveling wave autonomous laser [7], so that we can compare our previous experimental results with this model. Control of the standard Lorenz equations by modulation has previously been demonstrated by replacing the Rayleigh parameter R by $R[1 + \sin(\omega t)]$ [8–10]. Since we wish to model an autonomous laser with a modulated pump, we cannot use these

results as the transformation from the laser equations to the Lorenz equations assumes the pump is constant. Different transformations must be made, which do not involve R (see the Appendix). We show here that when the pump is modulated in our laser model, control to periodic behavior can be achieved. The total pump power is made to remain above the chaos threshold at all times, thus excluding a simple delayed bifurcation [11] as the control mechanism. In our recent experiments we modulated the laser so that the total pump power always remained above the chaos threshold [6].

II. THE COMPLEX LORENZ EQUATIONS

We investigate numerically the effect of modulating an optically pumped autonomous ring laser above the chaos threshold. We use the Lorenz equations to model the system, which is accurate for a two-energy-level system, or even a three-level system in certain parameter regimes [7]. Previous experiments have shown that an ammonia laser, which is an autonomous system, reproduces the same dynamics as the complex Lorenz equations [12]. The complex equations take into account the possibility that the cavity resonant frequency is detuned from the atomic resonance in general. By using this model we search for control to periodic pulsations that could be seen in autonomous lasers, and to investigate different types of locking ratios between the pump and laser output that may occur. The complex Lorenz equations are

$$\begin{aligned} \dot{E} &= -[(1 + i\delta)E - \lambda P], \\ \dot{P} &= -1/\sigma[(1 - i\delta)P - ED], \\ \dot{D} &= \beta/\sigma[1 - D + f(t) - \frac{1}{2}(E^*P + P^*E)], \\ \sigma &= \kappa/\gamma_{\perp}, \quad \beta = \gamma_{\parallel}/\gamma_{\perp}, \end{aligned} \tag{1}$$

where E , P , and D are the electric field, polarization, and inversion, respectively δ is the detuning of the cavity resonance relative to the atomic line center; κ , γ_{\perp} , and γ_{\parallel} are the electric field, polarization, and inversion decay rates, respectively λ is the average pump and $f(t)$ is the modulation applied to the pump. In our case $f(t) = A \sin(\omega t)$; and for

*Electronic address: kociuba@physics.uq.edu.au

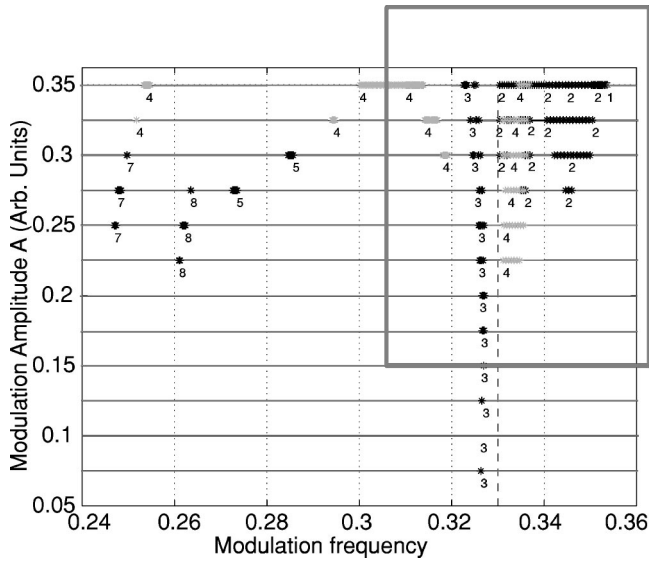


FIG. 1. Control to different periods with various combinations of ω and A . Dark points represent control to the period shown by the number near the points. The light gray band indicates the numerical grid, 1200×12 . The vertical dashed line represents the average frequency (of 0.33 units corresponding to the scaled time κt as shown at the end of the Appendix) of the unmodulated chaos where $A=0$ along this whole line. The gray box indicates the region where higher resolution calculations were performed, as shown in Fig. 3

chaos to occur, $\kappa > \gamma_{\parallel} + \gamma_{\perp}$. This is known as the bad cavity condition since a lossy cavity is required. The pump parameter is written in the form

$$I_p(t) = \lambda [1 + A \sin(\omega t)], \quad (2)$$

where λ is chosen such that $\lambda - A > \lambda_{ch}$, where λ_{ch} is the chaos threshold. Thus the pump parameter I_p is always above the chaos threshold. Since the energy into the laser is varying, this directly effects the population inversion. Previous work has been done using the standard Lorenz equations where the pump parameter λ was replaced by $\lambda [1 + A \sin(\omega t)]$ [9]. Unfortunately, we cannot use this as a correct description of modulation applied to a laser, as the inversion is not directly modulated in their case. Other authors have theoretically found control [8,13] using the appropriate form of the modulation for our laser, however, the total pump power was below the chaos threshold at certain times, i.e., there is a t_1 and t_2 such that $\lambda [1 + A \sin(\omega t)] < \lambda_{ch}$ for $2n\pi t_1 < t < 2n\pi t_2$, where n is any integer. This means that there is a periodic crossing of the bifurcation point. It has been shown that such a crossing can result in stabilization [11]. Here we ensure that $\lambda [1 + A \sin(\omega t)] > \lambda_{ch}$ for all t so that this mechanism is not the cause of control.

To ensure that the modulated system was initially chaotic, we integrated Eq. (1) in the deep chaotic regime where $\lambda = 46$ and $A = 0$ (no modulation).

Figure 1 shows the period of the signal for pairs of ω and A . An integration mesh of 1200 points on the ω axis and 12 points on the A axis was used, since the sensitivity of the system to ω was much greater than to A . Figure 1 shows

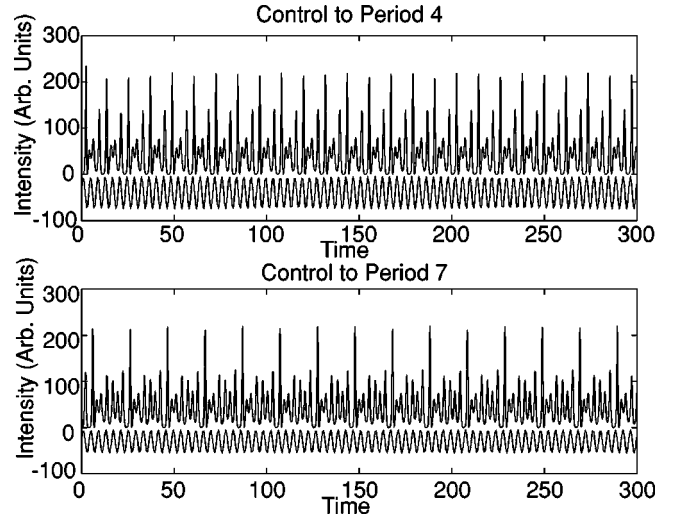


FIG. 2. Two numeric intensity time traces of control to periods 4 and 7, respectively, with locking ratios 3/4 and 5/7, respectively, using typical initial conditions. The lower trace in both cases is the modulation, the top trace is the intensity $E^*(t)E(t)$. The time units are scaled to the cavity decay rate κ as shown at the end of the Appendix. To check for stability we integrated both time traces up to a time of 1500 and found that the solution remained periodic.

there are islands of periodic response to modulation at various frequencies and amplitudes of modulation.

Period 3 dominates the graph near the average pulsation frequency of the unmodulated system shown as a vertical dashed line. The locking ratio, which is the ratio of the pump modulation frequency (ω) to the average pulsation frequency of the intensity, is 1/1 around this line, and p/q further away from this line, where p and q are integers. The island of period 4 centered around the frequency 0.33 has a locking ratio of 3/4. On the far left of the graph there is an island of control to period 7, which has a locking ratio of 5/7. Both of these states of control were found in our recent experiments [6]. The two corresponding (numeric) time traces show control to period 4 and period 7 in Fig. 2 using typical initial conditions. The lower trace in both plots is the term $A \sin(\omega t)$. The graph shows that the phase between the pump modulation and the output intensity is fixed and commensurate, since every 3 and 5 cycles of the pump for the upper and lower traces, respectively, brings the output intensity back to the start of period 4 and 7, respectively. Further analysis of Fig. 1 shows that the modulation frequency affects the average pulsation frequency, even though the average power from the modulation remains fixed at the value λ . For example, period 1 shown in the top far right of Fig. 1 is locked in a 1/1 ratio with the pump, yet the locked frequency is higher than the unmodulated chaos frequency by about 10%. Figure 1 spans a large range of parameter space, so we calculated the periodicity for a particular initial condition over a narrower parameter range indicated by the gray box in Fig. 1, at a much higher resolution. Figure 3 shows the result. Increasing the density of the integration mesh has revealed dynamics not seen in the previous calculation. For example, a modulation amplitude of 0.25 in Fig. 1 only shows control to period 3; however, in addition to period 3, Fig. 3 shows

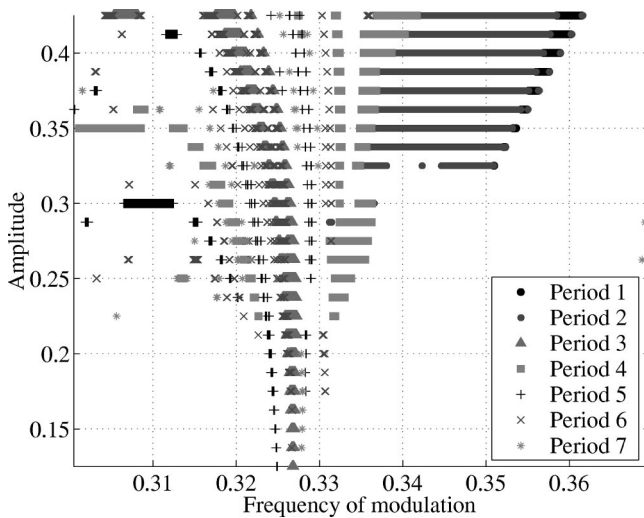


FIG. 3. Control to different periods with various combinations of ω and A . The frequency corresponds to the scaled time κt .

periods 4, 5, 6, and 7 with a significantly narrower window of control in modulation frequency space than for period 3. All the periods in this figure have a locking ratio of 1/1. This result shows there are even more closely spaced unstable periodic orbits that have been controlled to a periodic state.

Experimentally we found control to periods 1, 3, 4, and 7 with locking ratios of 1/1, 1/1, 3/4, and 5/7, respectively [6]. The amplitudes of modulation in all cases was 20%. The numerical model agrees well with control to period 3, but the amplitudes of modulation required for control are higher for periods 4, 7, and 1 where these are 60%, 50%, and 70%, respectively. Since we only use 2000 initial conditions, it is possible that there are other initial conditions lying on the chaotic attractor, which would lead to periodic behavior at a lower modulation amplitude.

We now investigate the Lyapunov dimension calculated using the Lyapunov exponents [14] of the stabilized orbit caused by the modulation of the pump. The dimension of the complex Lorenz system studied here is about 3.1. If the modulation frequency is not a harmonic of the pulsation frequency of the unmodulated laser, or the modulation amplitude is too low, the dimension remains at about 3.1 as can be seen by the gray lines in Figs. 4 and 5. When a periodic state is found, the dominant Lyapunov exponent changes from a positive value to zero. All other eigenvalues are negative. If the limit cycle is one dimensional, then there will be only one Lyapunov exponent of value zero, and the others will be negative. For a two-dimensional limit cycle (two-torus attractor) there will be two zero-valued Lyapunov exponents, and for a three-dimensional limit cycle there will be three zero-valued Lyapunov exponents. We find these types of limit cycles occur in our numerical results. Figure 4 shows control to period 4, and where chaos remains as a function of modulation amplitude and frequency. The modulation has a much larger impact on the dynamics of the system at the fundamental pulsation frequency (0.33) than at the rational harmonic $(3/4)f_0$ (at approximately 0.25). This is most clearly seen by observing how the dimension of the chaos changes with amplitude and frequency in both cases. At the

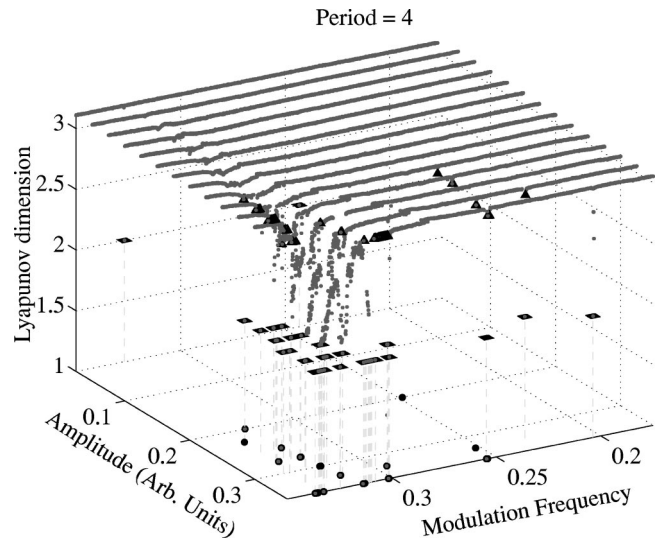


FIG. 4. A plot of the Lyapunov dimension of the modulated system for different pairs of modulation frequency and amplitude. The chaotic regions are of dimension 3.1 and are indicated by the gray lines. The controlled system to period 4 has integer dimension and is indicated by the black triangles, squares, and circles, which represent dimensions 3, 2, and 1, respectively. The frequency corresponds to the scaled time κt .

fundamental, the dimension of the chaos, even at small modulation amplitudes, drops slightly below 3.1 at the fundamental pulsation frequency. This slight drop in dimension becomes progressively deeper while approaching 3.0. Once it reaches 3.0 then the system is controlled to a periodic state indicated by triangles in the figure. At the modulation frequency of 0.25, no such behavior in the chaos occurs. It remains basically unchanged until the appropriate amplitude is reached, then the dimension drops suddenly to 3.0 and the system is controlled. Notice that the dimension of the stabi-

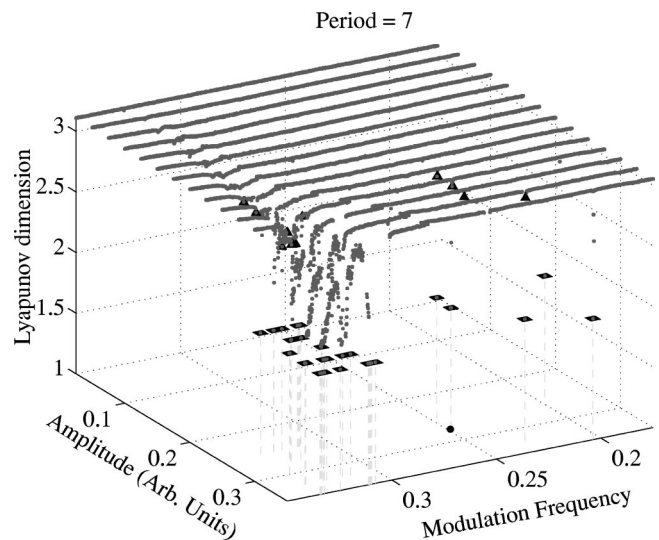


FIG. 5. A plot of the Lyapunov dimension of the modulated system for different pairs of modulation frequency and amplitude, as in Fig. 4 but for period 7. The frequency corresponds to the scaled time κt .

lized system can change to 3, 2 or 1. Dimension 3 appears first, followed by 2 and 1 confined within a narrow parameter space. At fixed amplitude, the dimension of the controlled system depends on the modulation frequency. There is some maximum width of modulation frequency around 0.33, which gives control; outside this range the system is chaotic. Figure 5 shows similar behavior except that control to period 7 with a dimension of 1 is very rare, but dimension 2 is most common. This is in contrast to Fig. 4 where there were comparable amounts of control to dimensions 1, 2, and 3.

We now investigate the dependence of control on the initial conditions. We calculated a numerical solution to Eq. (1) without modulation ($A=0$), and took 2000 (sequential) points lying on the chaotic attractor as the initial conditions for the system under modulation ($A \neq 0$). We do this as we assume the modulated system is initially free from modulation for a period of time such that the points in phase space lie on the attractor of this unmodulated system. The modulated system was integrated using the 2000 initial conditions, and for each initial condition we integrated the equations for different pairs of parameters ω (the modulation frequency) and A (the amplitude). For these pairs of parameters and initial conditions, the periodicity of $E^*(t)E(t)$, the intensity, was calculated. The solution was defined as periodic if a particular initial condition \mathbf{x}_i and its neighbor \mathbf{x}_{i+1} or \mathbf{x}_{i-1} also gave a periodic solution. We found that if this did not hold then the solution is not really periodic, as these points do not give periodic solutions when slight modifications are made to the integration routine. In the former case the solutions remain periodic. The periodicity of the signal was then calculated using the last half of the intensity time trace, thus ignoring any transient behavior that may have occurred.

Not all the points lying on the initially chaotic attractor ended up on the limit cycle generated by the application of the modulation. Of the 2000 initial conditions used, only a small subset of these points ($<5\%$) leads to control for a particular modulation frequency and amplitude. One should note that these initial conditions cover only a very small part of the five-dimensional chaotic attractor, so a more exhaustive coverage is required to make strong claims about basins of attraction, but is computationally intractable as many millions of initial conditions would be required.

Figure 6 is a plot of the locking ratio as a function of the applied modulation frequency. Each point on the graph corresponds to one of three amplitude values, $A=0.25$, 0.275 , and 0.3 , which are not distinguished in the figure. The scattered points represent uncontrolled states as the locking ratio is not rational. The gray lines represent control to period 7 at amplitudes $A=0.25$, 0.275 , and 0.3 , which is marked on the figure. These lines correspond to a locking ratio of $5/7$. All points on the graph correspond to particular initial conditions, which in general are different from each other, but some are the same. This information cannot be extracted from the figure. Control is not uniquely determined by modulation frequency and amplitude alone. This is evident in Fig. 6 by considering the modulation frequency 0.248 and amplitude marked 0.275. The gray band corresponds to control as mentioned above, however, some of the scattered points below this line also correspond to an amplitude of

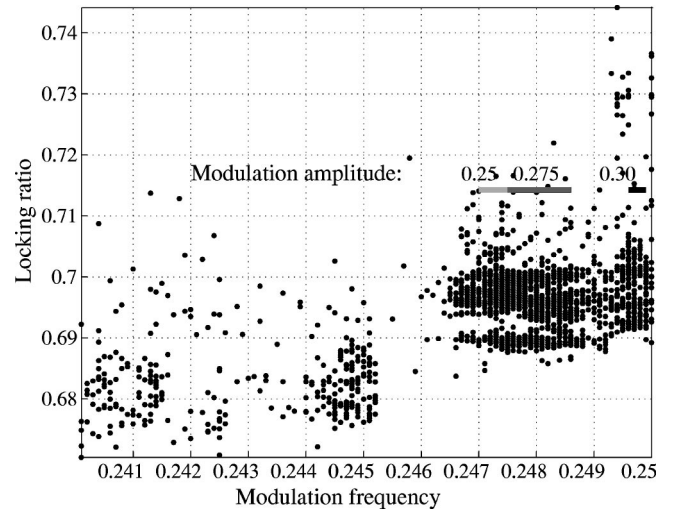


FIG. 6. Projection of the four variables: locking ratio, modulation frequency, amplitude, and initial conditions to locking ratio vs modulation frequency. Only the amplitudes $A=0.25$, 0.275 , and 0.30 during control to period 7 are labeled. Other points are a mixture of these three amplitudes and different initial conditions. Scattered points show uncontrolled behavior while a solid line represents control to period 7. Notice the scattered points below the dark lines, which shows that modulation frequency and amplitude are not enough to control the system, since the only difference between the line and points here is the initial conditions. The frequency corresponds to the scaled time κt .

0.275 (not evident in the figure). These points do not correspond to control as the locking ratio is not rational. Thus, only some of the initial conditions lead to control. The gray lines of control have a length that is determined by the combination of the maximum allowed frequency deviation from the center for fixed initial conditions and the maximum frequency deviation for a range of adjacent initial conditions. Now if the frequency is shifted further, control to period 7 is lost for all initial conditions and amplitudes tested. The resulting locking ratio for each initial condition in this case will vary from 0.67 to 0.7 as can be seen at frequency 0.241.

III. CONCLUSION

We have shown that the complex Lorenz equations describing a chaotic autonomous laser can be controlled to a periodic state by modulating the pump parameter appropriately. We find that there exist islands of control to various periods in modulation amplitude-frequency parameter space. These islands are accessed only for a subset of the initial conditions that were used. The width of control in frequency space is quite narrow, but increases with increasing modulation amplitude. Control is not as sensitive to the modulation amplitude, although increasing the amplitude sufficiently can change the period of control. The nonlinearity of the system has been successfully exploited since rational locking ratios of the pump to intensity output gave control. We have found similar behavior in the experimental results we obtained using a chaotic autonomous ammonia laser.

APPENDIX

Starting with the Maxwell-Bloch equations,

$$\begin{aligned}\dot{E} &= -\kappa(1+i\delta)E - \frac{i\omega_c}{2\epsilon_0}P, \\ \dot{P} &= -\gamma_{\perp}(1-i\delta)P - \frac{iU^2}{\hbar}ED, \\ \dot{D} &= -\gamma_{\parallel}(D-D_0) - \frac{1}{2i\hbar}(E^*P - P^*E),\end{aligned}\quad (\text{A1})$$

we make the transformation,

$$E = \frac{-\hbar}{i\nu_{12}}\sqrt{\gamma_{\parallel}\gamma_{\perp}}E', \quad (\text{A2})$$

$$P = -2\sqrt{\gamma_{\parallel}\gamma_{\perp}}\frac{\epsilon_0\hbar\kappa}{\omega_c\nu_{12}}P', \quad (\text{A3})$$

$$D = \frac{2\epsilon_0\hbar\kappa\gamma_{\perp}}{\omega_c U^2}D'. \quad (\text{A4})$$

Here $U^2 = \nu_{12}\nu_{12}^*$, and $\delta = (\omega - \omega_c)/\kappa$. The lasing frequency is pulled to ω , and ω_c is the empty cavity frequency. This gives

$$\dot{E}' = -\kappa[(1+i\delta)E' - P'], \quad (\text{A5})$$

$$\dot{P}' = -\gamma_{\perp}(1-i\delta)P' + \gamma_{\perp}E'D', \quad (\text{A6})$$

$$\dot{D}' = -\gamma_{\parallel}\left(D' - D_0\frac{\omega_c U^2}{2\epsilon_0\hbar\kappa\gamma_{\perp}}\right) - \gamma_{\parallel}(E'^*P' + P'^*E'). \quad (\text{A7})$$

Modulating the pump power will lead to a modulation of the population inversion, so we write $D_0 = D_{ss}[1 + f(t)]$, substituting λ as

$$\lambda = \frac{\omega_c U^2}{2\epsilon_0\hbar\kappa\gamma_{\perp}}D_{ss}. \quad (\text{A8})$$

Thus Eq. (A7) becomes

$$\dot{D}' = -\gamma_{\parallel}[D' - \lambda(1 + f(t))] - \gamma_{\parallel}(E'^*P' + P'^*E'). \quad (\text{A9})$$

Finally, transforming only the static part of the pump

$$E' = E,$$

$$P' = \lambda P,$$

$$D' = \lambda D, \quad (\text{A10})$$

and rescaling time $t = \tau = \kappa t$ transforms the decay rates and the result is Eq. (1).

-
- [1] J.P. Eckmann and D. Ruelle, *Rev. Mod. Phys.* **57**, 617 (1985).
 [2] E. Ott, C. Grebogi, and J.A. Yorke, *Phys. Rev. Lett.* **64**, 1196 (1990).
 [3] C. Liu, R. Roy, H.D.I. Abarbanel, Z. Gills, and K. Nunes, *Phys. Rev. E* **55**, 6483 (1997).
 [4] S. Boccaletti, D.L. Valladares, J. Kurths, D. Maza, and H. Mancini, *Phys. Rev. E* **61**, 3712 (2000).
 [5] Y. Braiman and I. Goldhirsch, *Phys. Rev. Lett.* **66**, 2545 (1991).
 [6] G. Kociuba, N.R. Heckenberg, and A.G. White, *Phys. Rev. E* **64**, 056220 (2001).
 [7] R. Gilmore, R. Vilaseca, R. Corbalan, and E. Roldan, *Phys. Rev. E* **55**, 2479 (1997).
 [8] J. Bhattacharjee, K. Banerjee, D. Chowdhury, and R. Saravanan, *Phys. Lett.* **104A**, 33 (1984).
 [9] Y. Liu and J.R.R. Leite, *Phys. Lett. A* **185**, 35 (1991).
 [10] K.A. Mirus and J.C. Sprott, *Phys. Rev. E* **59**, 5313 (1999).
 [11] H. Zeghlache and P. Mandel, *J. Opt. Soc. Am. B* **2**, 18 (1985).
 [12] C. Weiss, R. Vilaseca, N. Abraham, R. Corbalan, E. Roldan, and G. de Valcarcel, *Appl. Phys. B: Lasers Opt.* **B61**, 223 (1995).
 [13] T. Ogawa and E. Hanamura, *Appl. Phys. B: Photophys. Laser Chem.* **B43**, 139 (1987).
 [14] J. L. Kaplan and J. A. Yorke, *Functional Differential Equations and Approximation of Fixed Points* (Springer, Berlin, 1979), p. 204.